ANL/ET/CP--86340
CONF-9510225--3

ANALYSIS OF BORON DILUTION IN A FOUR-LOOP PWR*

RECEIVED
JAN 24 1995
OSTI

by

J. G. Sun and W. T. Sha
Energy Technology Division
Argonne National Laboratory
9700 South Cass Avenue
Argonne, Illinois 60439

Submitted to Specialist Meeting on Boron Dilution Reactivity Transients
October 18–20, 1995, State College, PA

*Work sponsored by U.S. Nuclear Regulatory Commission

DISCLAIMER

Portions of this document may be illegible in electronic image products. Images are produced from the best available original document.

ANALYSIS OF BORON DILUTION IN A FOUR-LOOP PWR

J. G. Sun and W. T. Sha

Energy Technology Division
Argonne National Laboratory
9700 South Cass Avenue
Argonne, IL 60439

Abstract

Thermal mixing and boron dilution in a pressurized water reactor were analyzed with COMMIX codes. The reactor system was the four loop Zion reactor. Two boron dilution scenarios were analyzed. In the first scenario, the plant is in cold shutdown and the reactor coolant system has just been filled after maintenance on the steam generators. To flush the air out of the steam generator tubes, a reactor coolant pump (RCP) is started, with the water in the pump suction line devoid of boron and at the same temperature as the coolant in the system. In the second scenario, the plant is at hot standby and the reactor coolant system has been heated up to operating temperature after a long outage. It is assumed that an RCP is started, with the pump suction line filled with cold unborated water, forcing a slug of diluted coolant down the downcomer and subsequently through the reactor core. The subsequent transient thermal mixing and boron dilution that would occur in the reactor system is simulated for these two scenarios. The reactivity insertion rate and the total reactivity are evaluated.

1 Introduction

A number of mechanisms that have been postulated lead to reactivity–induced transients through boron dilution in a pressurized water reactor (PWR). One mechanism is to quickly pump a slug of cold unborated water through the core, and cause insertion of positive reactivity and thus power excursion and fuel damage. The most conservative assumption in terms of reactivity insertion is that the cold unborated inlet water does not mix with the hot boron–rich water initially in the reactor vessel and the reactor coolant pipes. Therefore, the extent of mixing of cold unborated water with hot boron–rich water is important in realistically quantifying the reactivity insertion due to thermal mixing and boron dilution.

Thermal mixing and boron dilution in the four-loop Zion reactor[1] were analyzed with COMMIX codes.[2–5] COMMIX is a general–purpose, time–dependent, multidimensional computer code for thermal hydraulic analysis of single– or multicomponent engineering systems. It solves a system of conservation equations of continuity, momentum, and energy, and a k–ε two–equation turbulent model. A special feature of the COMMIX code is its porous–media formulation, which represents an unified approach to thermal–hydraulic analysis. A three–dimensional numerical model, based on Cartesian coordinates, was developed for the four–loop reactor system.[6] The major objective of these analyses was to determine the reactivity insertion due to the change of coolant density and boron concentration in the reactor core.

Two boron dilution scenarios were analyzed. In the first scenario, the plant is in cold shutdown and the reactor coolant system has just been filled after maintenance on the steam generators. To flush the air out of the steam generator tubes, a reactor coolant pump (RCP) is started. It is assumed that the coolant in the pump suction line (crossunder line that connects the RCP suction to the outlet of the steam generator) is at the same temperature as the coolant in the system but is devoid of boron. The COMMIX simulation for this scenario is referred to as isothermal–RCP–start calculation.

In the second scenario, it is assumed that all RCPs are recently tripped, and conditions for a restart have been met. The plant is at hot standby and the reactor coolant system has been heated to operating temperature after a long outage. Therefore, natural circulation does not exist because adequate decay heat is lacking. This condition will lead to stagnation of the coolant in the reactor system. It is assumed that boron dilution took place in one of the four pump suction lines during the outrage. When the RCP in the diluted loop is started (with the suction line filled with cold unborated water), a slug of diluted coolant will be forced down the downcomer and subsequently through the reactor core. This simulation is referred to as hot–RCP–start calculation.

In these two analyses, the transient flow and boron distribution, and, for the second analysis, the temperature distribution, are computed with the COMMIX code. The reactivity insertion due to the boron dilution and the density change is then estimated.

2 Layout of Four–Loop Zion Reactor

The Zion reactor was selected as the model PWR because it has previously been modeled by COMMIX.[6] It is a typical four–loop PWR with a capacity of 1000 MW. Figure 1 shows a top view of the plant layout, and Fig. 2 shows a side view of the plant layout. The layout of the internal structures of the Zion reactor vessel is illustrated in Fig. 3.

At normal operation, inlet coolant flow from the cold leg enters the vessel inlet nozzles and proceeds down the annulus between the core barrel and the vessel wall, flows on both sides of the thermal shield, and then into the plenum at the bottom of the vessel. It then turns and flows up through the lower support plate, passes through the intermediate diffuser plate and through the lower core plate. After passing through the core, the coolant enters the area of the upper support structure and then flows generally radially to the outlet nozzles of the core barrel and directly through the vessel outlet nozzles to the hot leg.

A small amount of water also flows between the baffle plates and core barrel. Similarly, a small amount of the entering flow is directed into the vessel head plenum. Both these flows eventually are directed into the upper support structure plenum and exit through the vessel outlet nozzles to the hot leg.

3 The Numerical Model

3.1 Geometry

The numerical model of the four–loop Zion reactor coolant system is an extension of the one–loop model developed in Ref. 1. A schematic layout of the three–dimensional model for one loop is shown in Fig. 4. A top view of the model is shown in Fig. 5. The model contains 20 x 28 horizontal partitions and 20 vertical partitions, for a total of 3334 computational cells.

The vertical partitions of the model shown in Fig. 6 correspond to the major components of the reactor vessel, as illustrated in Fig. 3. From Figs. 3 and 6 it is evident that most of the axial partitions match in a natural way. The axial height of the upper and lower domes of the reactor vessel were adjusted to ensure correct fluid volume. The horizontal dimensions of the grids were determined from the cross–sectional areas of the major components and from the areas between the components.

The steam generators are partitioned to preserve the height and flow areas. All circular pipes, i.e., cold legs, hot legs, and crossunder lines, are modeled with rectangular cross sections. The cross–sectional areas of the modeled pipes are the same as those of the corresponding circular pipes.

To account for the surfaces and volumes occupied by the solid structures in the flow domain, the directional surface porosity and the volume porosity are specified for various components. The directional surface porosity used in the COMMIX code is defined by the equation

$$\gamma_{x_i} = \frac{\text{Fluid flow area in direction } x_i}{\text{Total area in direction } x_i},$$

and the volume porosity is defined by

$$\gamma_v = \frac{\text{Fluid volume of a cell}}{\text{Total volume of a cell}}.$$

3.2 Flow resistances

To account for the frictional resistance of the solid structures in the reactor vessel, a set of seven resistance correlations of the form

$$f = a_l \, Re^{b_l} + c_l \qquad \text{(for laminar flow)}$$

$$= a_t \, Re^{b_t} + c_t \qquad \text{(for turbulent flow)}$$

has been implemented in the model. In these correlations, a, b, and c are correlation coefficients, Re is the Reynolds number, and f is the friction factor. These correlations are used to compute frictional resistances in the x, y, and z directions in the reactor core, core bypass, upper plenum, upper plenum bypass, upper core plate, and in steam generators.

3.3 Heat transfer to walls

The core power and heat capacity of both the reactor and pipe walls were not considered in this model. However, they can easily be implemented. We believe these effects are of secondary importance in terms of assessing reactivity insertion due to thermal mixing and boron dilution.

3.4 Fluid physical properties

In the analyses, boron and water are treated as separate components. Because the boron concentration in the system is very small, the thermophysical property of the boron/water mixture is essentially the same as that of unborated water.

3.5 Initial Conditions

For the isothermal–RCP–start calculation, the reactor coolant system was initially filled with borated water at 25°C, 155 bars, and zero velocity. A boron concentration of 2200 ppm, corresponding to a mass fraction of 1.32×10^{-3}, was uniformly distributed in the entire reactor coolant system.

For the hot–RCP–start calculation, the reactor coolant system was initially filled with borated water at 297°C, 155 bars, and zero velocity. A boron concentration of 1200 ppm, corresponding to a mass fraction of 7.209×10^{-4}, was uniformly distributed in the entire reactor coolant system.

3.6 Boundary Conditions

The inlet is at the suction side of the RCP in the second loop, as shown in Fig. 5. The inlet conditions for the two calculations, the isothermal– and the hot–RCP–start, are listed below.

(1) In the isothermal–RCP–start calculation, we assume that a slug of unborated water, initially in the crossunder pipe and half the volume of the RCP, is pumped into the cold leg in Loop 2. The temperature of the inlet water is the same as that in the system. The volume of the slug is 4.87 m^3 (168.9 ft^3), and the increase of pump flow rate with time is shown in Fig. 7.[1] The pump reaches its normal operating flow rate of 130,000 gpm in 25 s. From Fig. 7, it can be determined that the slug of cold unborated water will pass through the pump in 8 s. After 8 s, the boron concentration in the inlet water becomes normal (2200 ppm).

(2) In the hot–RCP–start calculation, the temperature of the inlet slug is low, i.e. 25°C. The unborated slug has the same volume as that in the above calculation. After the slug passes through the pump, boron concentration at the inlet returns to 1200 ppm, and the temperature to 297°C, which is the initial temperature of the system.

It should be noted that in these two calculations, the slug water is assumed only in Loop 2. There is no boron dilution in the other three loops and those RCPs are assumed open for coolant pass through.

The outlet is located at the exit side of the steam generator in the second loop, as shown in

Fig. 5. The velocity and temperature gradients at the outlet were set to zero, i.e.,

$$\frac{\partial u_z}{\partial z} = 0, \qquad \frac{\partial T}{\partial z} = 0.$$

Velocity and heat flux were zero on the surfaces of all solid walls.

4 COMMIX Calculational Results

4.1 Boron Dilution under Isothermal–RCP–Start Condition

The transient of the boron dilution in the four–loop reactor coolant system is simulated for 35 s. At 35 s into the transient, most of the slug has been pushed out of the reactor vessel. Figures 8a–d show the velocity distributions in the cold legs (Loops 1 and 2) and reactor vessel at 6, 9, 13, and 18 s into the transient, respectively. At 6 and 9 s into the transient, the inlet velocity is lower. Water in the reactor core and lower plenum is simply pushed upward with nonuniform velocity distribution. At 13 s into the transient, a small recirculation can be observed at the left corner in the lower plenum, Fig. 8c. Flow recirculation commonly occurs at high flow rates, or at high Reynolds numbers. At later times, the magnitude of the recirculating velocity increases, as shown in Fig. 8d for 18 s into the transient. Although not seen in Figs. 8a–d, large flow recirculations are observed in the downcomer. These flow recirculations will improve the boron mixing in the reactor vessel.

The inlet flow is bypassed in the loops. In Loop 2, water flows from the reactor vessel to the hot leg and then to the steam generator. In Loops 1, 3, and 4, however, the flow is reversed. This reversal occurs because only the RCP in Loop 2 is running, and the other loops become bypass routes for the inlet flow. The bypass flow reduces the volume of the slug flowing through the core and, therefore, mitigates the boron dilution in the core. The total bypass flow rate accounts for 20.6% of the inlet flow rate. It should be pointed out that the bypass flow rates depend on the modeling of the flow resistance in the steam generator and the pipes.

The inlet unborated water mixes with the boron–rich coolant in the system. The calculational result indicates that little boron mixing occurs in the cold leg. However, strong boron mixing occurs in the downcomer. For instance, at 14 s into the transient, the lowest boron concentration in the lower plenum is 1849 ppm. Therefore, after the downcomer, the boron concentration in the slug has recovered to ≈84% of the initial 2200–ppm boron concentration of the system. The strong mixing is due partially to the large volume of the downcomer and partially to the flow circulations in the downcomer. Additional mixing takes place in the lower plenum and in the reactor core, resulting in an increase of the minimum boron concentration to 2006 ppm in the core at 20 s into the transient. The travel of the slug through the core is shown in Figs. 9a–d, which show that the slug enters the core at ≈16 s and exits the core at ≈22 s into the transient. The figures also show that the boron concentration is not uniform at each level in the core.

Although the boron concentration is not uniform, a mean boron concentration at each horizontal level is helpful in estimating the overall boron dilution in the reactor vessel. The mean boron concentration as a function of vessel height z is shown in Fig. 10 for the transient at 16, 18, 20, and 22 s. Figure 10 also identifies the location of the slug and shows that the mean boron concentration in the core is always higher than 2046 ppm. Therefore, the mean boron concentration in the core is reduced by <154 ppm, or 7%, which indicates moderate mixing in the downcomer and lower plenum. In the most conservative estimation, by assuming no mixing, the boron concentration in the core would have been reduced to zero when the slug entered the core.

Let us denote the average boron concentration in the core as B, the mean rate of boron concentration change ($\Delta B/\Delta t$) can be obtained from Fig. 10. The reactivity insertion rate due to boron concentration change $\Delta K_B/\Delta t$ as a function of time is obtained by multiplying $\Delta B/\Delta t$ with the reactivity coefficient $\partial K_B/\partial B$. For the condition of this analysis, $\partial K_B/\partial B$ is 10.2×10^{-5} ppm^{-1}.[1] The variation of the reactivity insertion rate $\Delta K/\Delta t$ (= $\Delta K_B/\Delta t$) with time is plotted in Fig. 11. It is seen that the reactivity insertion rate in the core increases rapidly after 12 s into the transient and reaches a maximum of ≈0.0034 s^{-1} (1 pcm = 10^{-5} s^{-1}), or ≈\$0.76/s with the conversion factor β

= 0.0045, at 17.5 s into the transient. The total reactivity K is the integration of $\Delta K/\Delta t$ with time and it is also plotted in Fig. 11. The maximum mean reactivity is ≈0.014 (or ≈$3.1), which is high. Because of the nonuniformity of the boron distribution, the maximum local reactivity rate and reactivity are even higher. The local reactivity rate and reactivity represent the local power density change (or local temperature change with respect to time) and local power density (or local temperature), respectively.

4.2 Thermal Mixing and Boron Dilution under Hot–RCP–Start Condition

The transient of the thermal mixing and boron dilution in the reactor coolant system is simulated for 35 s. The overall velocity distributions are similar to those obtained in the isothermal calculation at corresponding times. However, because the temperature of the slug in this calculation is much lower than that of the water in the reactor vessel, local velocities change because of the buoyancy effect. The velocity of the local flow in the downcomer is greater. As a result, the cold unborated inlet slug will not mix well in the downcomer and in the lower plenum. The slug flows horizontally to the other side in the lower plenum and then turns upward. The total flow bypassed through Loops 1, 3, and 4 is 20.5% of the inlet flow in Loop 2.

Calculated temperature contours are plotted in Figs. 12a–d for 16, 18, 20, and 22 s into the transient. Near the slug front, the isotherms are approximately horizontal, as observed in Figs. 12a and 12b, indicating good mixing of the front portion of the slug in the lower plenum. Before the remainder of the slug is mixed, the larger inlet flow pushes it to the right corner in the lower plenum, as shown in Fig. 12a. The slug then rises at the right side, as shown in Figs. 12b–d.

The calculated distributions of boron concentration are similar to those of the temperature shown in Figs. 12a–d. The slug does not mix well with the vessel water in the downcomer because of the buoyancy effect, and in the lower plenum because of the short residence time. The minimum boron concentration in the lower plenum at 14 s into the transient is 902 ppm, ≈75% of the initial boron concentration, compared with 84% in the isothermal calculation. The mean boron concentration as a function of vessel height z is shown in Fig. 13 for the transient at 16, 18, 20, and 22 s. The mean boron concentration in the core is always >1025 ppm. The maximum decrease of the mean boron concentration in the core is 14.6%, compared with 7% in the isothermal calculation. Or, from the view point of boron mixing of the slug that was initially unborated, its boron concentration reached only to 85.4% of the initial boron concentration of the system in this calculation, whereas, in the isothermal case, it reached 93%. Therefore, the boron mixing for the slug in this calculation is worse than that in the isothermal calculation.

The total rate of reactivity insertion ($\Delta K/\Delta t$) is the sum of that due to the change in boron concentration ($\Delta K_B/\Delta t$) and that due to change in coolant density ($\Delta K_\rho/\Delta t$). The reactivity rate due to boron concentration change $\Delta K_B/\Delta t$ is obtained by multiplying the reactivity coefficient $\partial K_B/\partial B$ by $\Delta B/\Delta t$. The reactivity rate due to density change $\Delta K_\rho/\Delta t$ is the product of density change per second ($\Delta\rho/\Delta t$) multiplied by the reactivity coefficient due to density change ($\partial K_\rho/\partial\rho$). For the condition of this analysis, $\partial K_\rho/\partial\rho = 31.15\text{x}10^{-5}$ m^3/kg (or 0.00499 ft^3/lb).[1] The rate of change in coolant density ($\Delta\rho/\Delta t$) can be obtained by multiplying $\Delta T/\Delta t$ by $\partial\rho/\partial T$, which is -1.61 $kg/m^3/^\circ C$ for water. The variation of the total reactivity insertion rate in the core with time $\Delta K/\Delta t$ is plotted in Fig. 14. It is seen that the reactivity insertion rate in the core increases rapidly after 12 s into the transient and reaches a maximum of ≈ 0.0082 s^{-1} (or ≈$1.8/s) at 15.5 s into the transient. The variation of total reactivity K with time is also plotted in Fig. 14. The maximum reactivity is ≈0.029 (or ≈$6.4) at 18 s into the transient, which is very high. Again, because of the nonuniformity of boron distribution, the maximum local reactivity rate and reactivity are even higher.

5 Discussion and Conclusions

1. Transient calculations for thermal mixing and boron dilution in a four–loop PWR coolant system were performed with the COMMIX code. In the isothermal–RCP–start calculation, large

flow recirculations were found in the downcomer and small flow recirculations were found in the lower plenum of the reactor vessel. These flow recirculations improved the boron mixing of the unborated inlet slug with the coolant in the reactor vessel. As a result, there was strong boron mixing in the downcomer and moderate boron mixing in the lower plenum and reactor core. As the slug passed through the downcomer, its boron concentration recovered from 0 to 84% of the system boron concentration. Additional boron mixing took place in the lower plenum and reactor core. Furthermore, the bypass of the inlet flow through the other three loops (reverse flows) reduced the volume of the slug passing through the core. The total bypass accounted for 20.6% of the inlet flow rate. The mean reactivity insertion rate ($\Delta K/\Delta t$) increased quickly after 12 s into the transient and reached a maximum of $\approx 0.0034\ s^{-1}$, or ≈$0.76/s, at 17.5 s into the transient. The maximum reactivity K was ≈0.014 (or ≈$3.1) at 20 s into the transient, which is high.

2. In the hot–RCP–start calculation, boron mixing was not as good as that in the isothermal calculation. Although large flow recirculations existed in the downcomer, the flow was dominantly downward as the cold slug was passing through the downcomer, which was due to the buoyancy effect. As the slug passed through the downcomer, its boron concentration recovered from 0 to 75% of the system boron. It was also found that the cold slug does not have enough time to mix with the vessel coolant in the lower plenum. It was pushed to the opposite side of the inlet loop by the large inlet flow rate. Moderate thermal and boron mixing occurs in the lower plenum and in the reactor core. The total bypass accounted to 20.5% of the inlet flow rate. The mean reactivity insertion rate ($\Delta K/\Delta t$) due to both the coolant density change and boron concentration change also increased quickly after 12 s into the transient and reached a maximum of $\approx 0.0082\ s^{-1}$, or ≈$1.8/s, at 15.5 s into the transient. The maximum reactivity K was ≈0.029, or ≈$6.4, at 18 s into the transient, which is very high.

3. The results presented here appear reasonable. However, this was the first time we used the COMMIX code to predict boron concentration distribution. We are interested to validate our model with experimental boron dilution data.

4. The proper procedure to compute reactivity feedback due to boron dilution and thermal mixing is to perform an integral, time–dependent, three–dimensional, thermal–hydraulic–neutronic calculation. The present calculations are limited to time–dependent, three–dimensional, thermal–hydraulic calculations. Reactivity feedback due to boron dilution and thermal mixing is estimated via reactivity coefficients[1] with respect to change in boron concentration ($\partial K/\partial B$) and coolant density ($\partial K/\partial \rho$). These reactivity coefficients were very conservative values based on point kinetics.

5. The complex geometry of the four–loop Zion reactor has been greatly simplified and represented in Cartesian coordinates. Because a porous medium formulation is used in the COMMIX code, both volume and area occupied by fluid in each reactor component are correctly simulated via volume porosity and directional surface porosities. These simplification in geometrical representation in our numerical model will affect the flow field.

Acknowledgments

The authors gratefully acknowledge the encouragement and support of Gene Trager, George Lanik, and Jack Rosenthal of the Office for Analysis and Evaluation of Operational Data, U.S. Nuclear Regulatory Commission, and thank K. Ramsden, D. Redden, and S. Ahmend of Commonwealth Edison Company for useful discussions.

References

1. J. G. Sun, and W. T. Sha, *Analysis of Thermal Mixing and Boron Dilution in a PWR*, NUREG/CR–5822, Argonne National Laboratory Report ANL–91/43 (1993).

2. W. T. Sha, H. M. Domanus, R. C. Schmitt, J. J. Oras, and E. I. H. Lin, *COMMIX–1: A Three–Dimensional Transient Single–Phase Computer Program for Thermal–Hydraulic Analysis*, NUREG/CR–0785, Argonne National Laboratory Report ANL–77–96 (Sept. 1978).

3. H. M. Domanus, R. C. Schmitt, W. T. Sha, and V. L. Shah, *COMMIX–1A: A Three–Dimensional Transient Single–Phase Computer Program for Thermal–Hydraulic Analysis of Single and Multicomponent Systems: Vol. I User's Manual,* and *Vol. II Assessment and Verification*, NUREG/CR–2896, Argonne National Laboratory Report ANL–82–25 (Dec. 1983).

4. F. F. Chen, H. M. Domanus, C. C. Miao, R. C. Schmitt, V. L. Shah, and W. T. Sha, *COMMIX–1B: A Three–Dimensional Transient Single–Phase Computer Program for Thermal–Hydraulic Analysis of Single and Multicomponent Systems: Vol. I Equations and Numerics,* and *Vol. II User's Manual*, NUREG/CR–4348, Argonne National Laboratory Report ANL–85–42 (Sept. 1985).

5. H. M. Domanus, Y. S. Cha, T. H. Chien, R. C. Schmitt, and W. T. Sha, *COMMIX–1C: A Three–Dimensional Transient Single–Phase Computer Program for Thermal–Hydraulic Analysis of Single and Multicomponent Engineering Systems: Vol. I Equations and Numerics,* and *Vol. II User's Manual*, NUREG/CR–5649, Argonne National Laboratory Report ANL–90/33 (Nov. 1990).

6. V. L. Shah, *Thermal Hydraulic Simulation of Zion Power Plant under Normal Operating Conditions*, Argonne National Laboratory Report ANL/ATHRP-36 (1985).

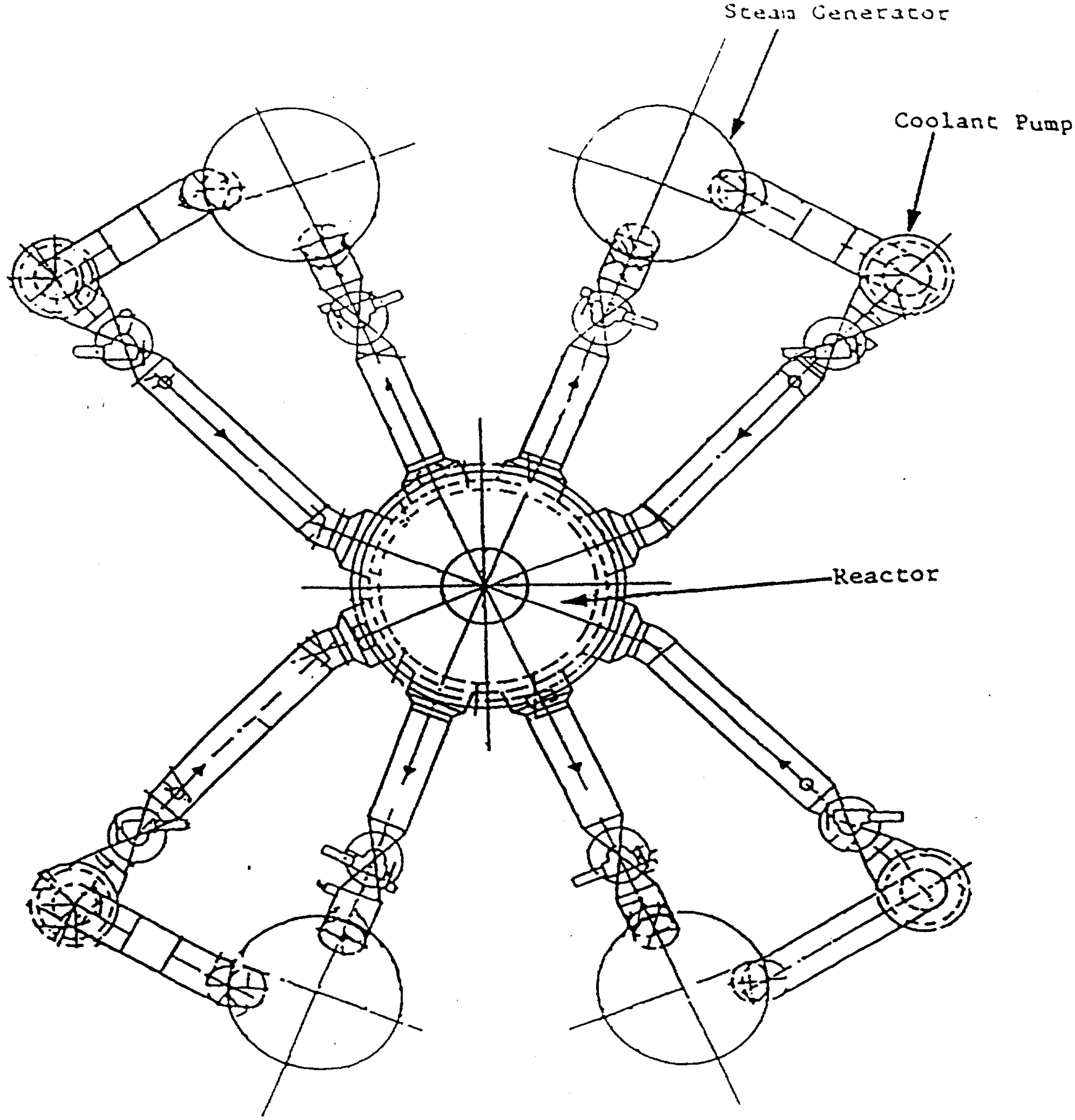

Fig. 1. Top view of layout of Zion reactor coolant loops

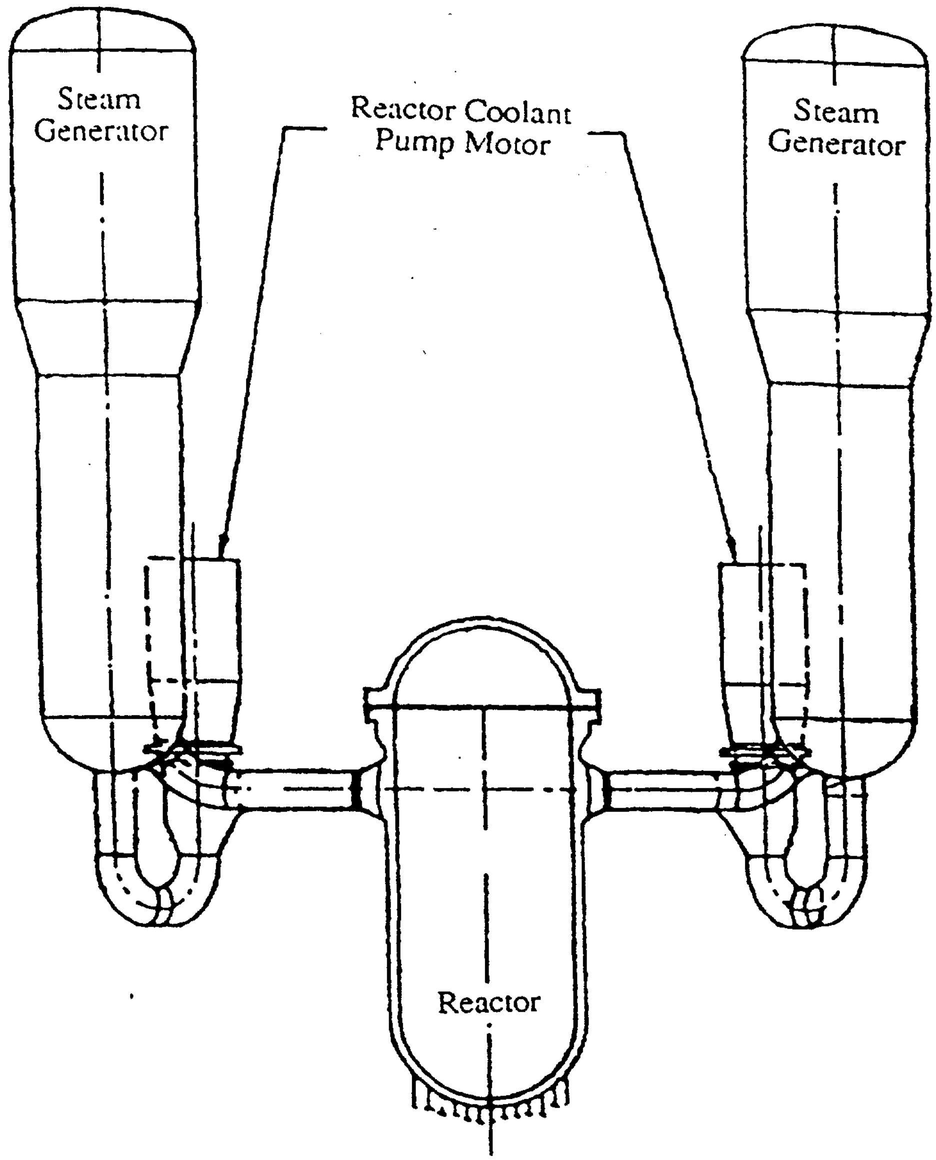

Fig. 2. Side view of layout of Zion reactor coolant loops

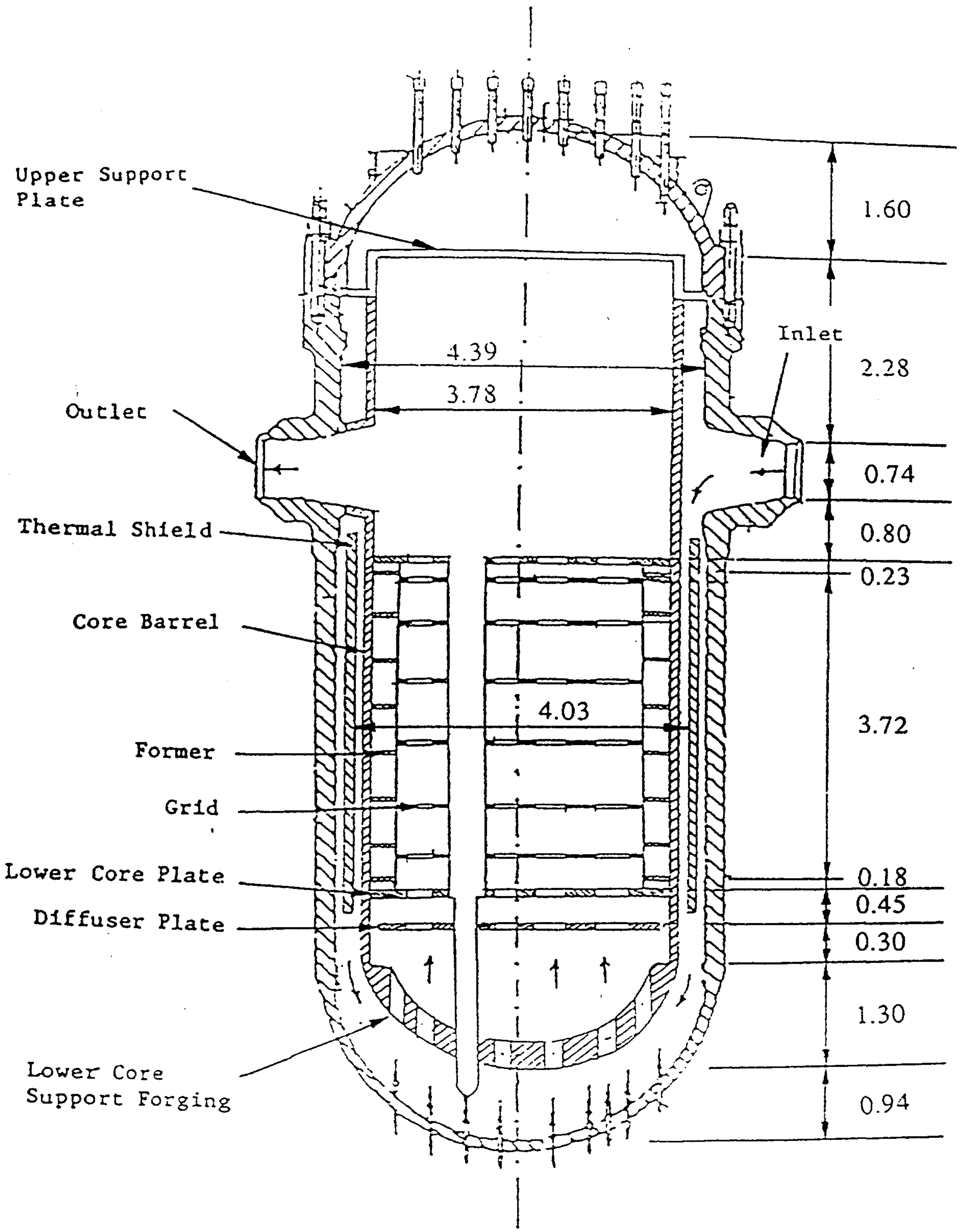

Fig. 3. Schematic layout of internal structures of Zion reactor (Dimensions in meters)

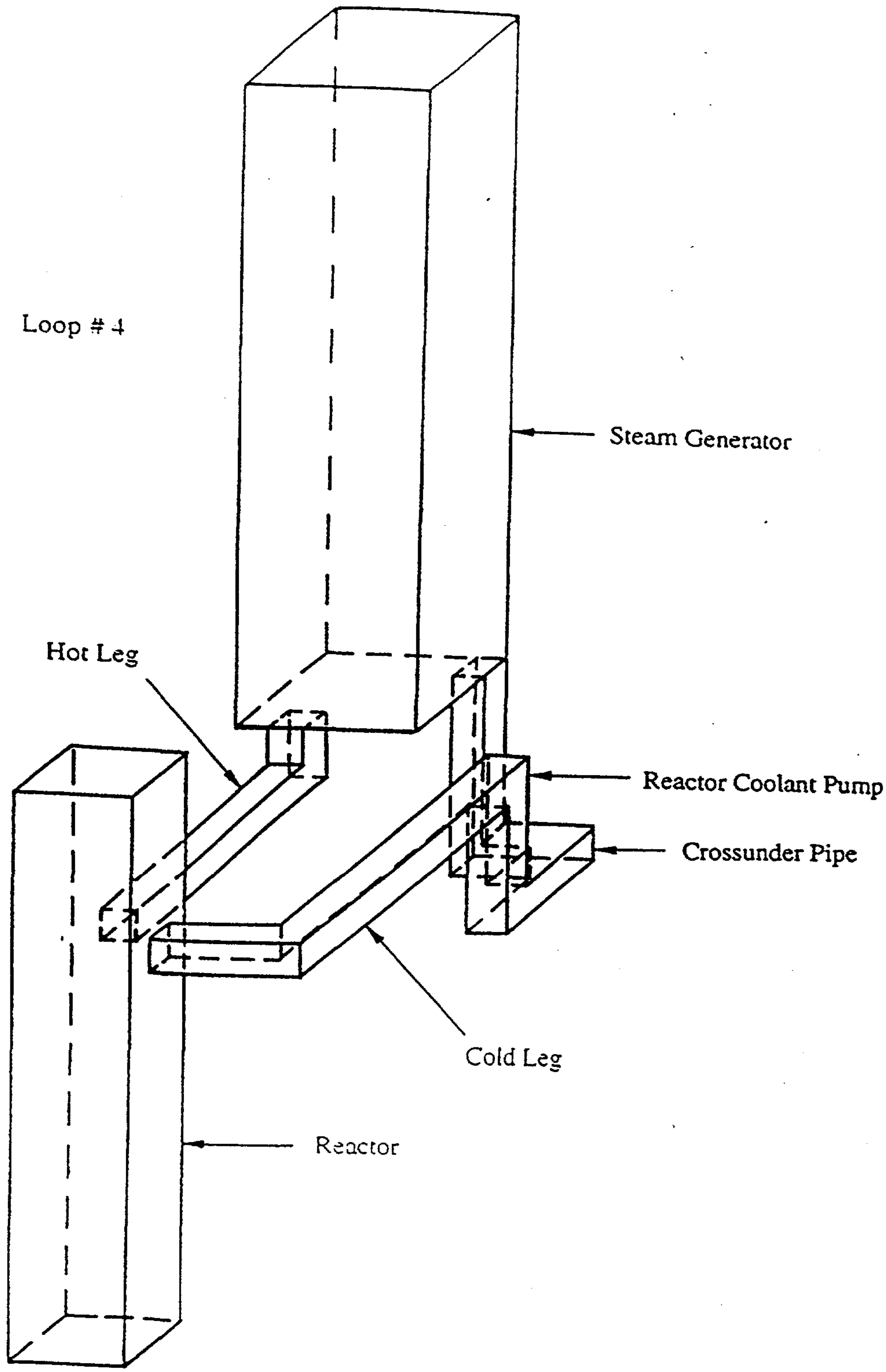

Fig. 4. Schematic layout of three-dimensional model for Zion reactor Loop 4

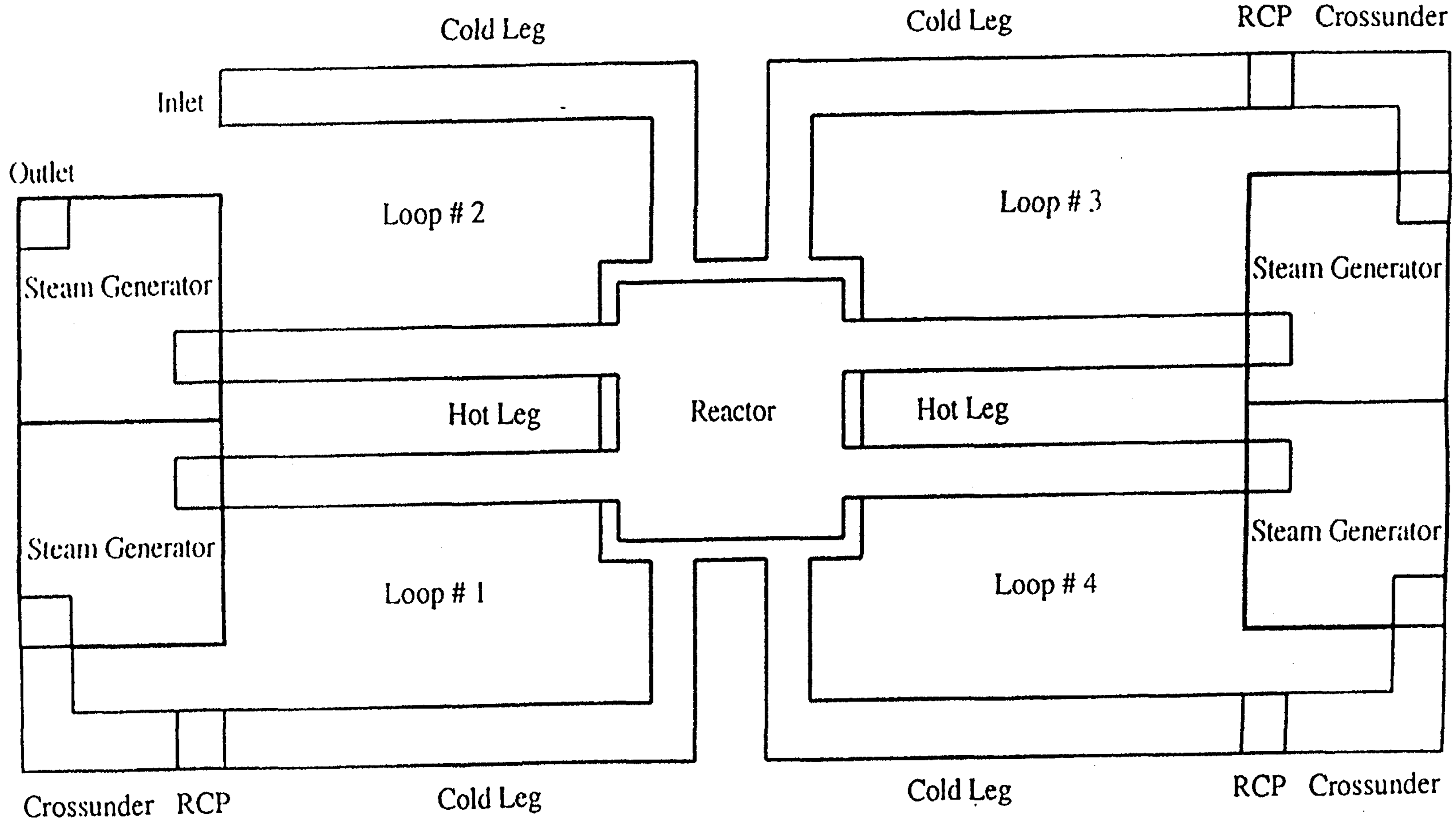

Fig. 5. Top view of numerical model of Zion reactor coolant loops

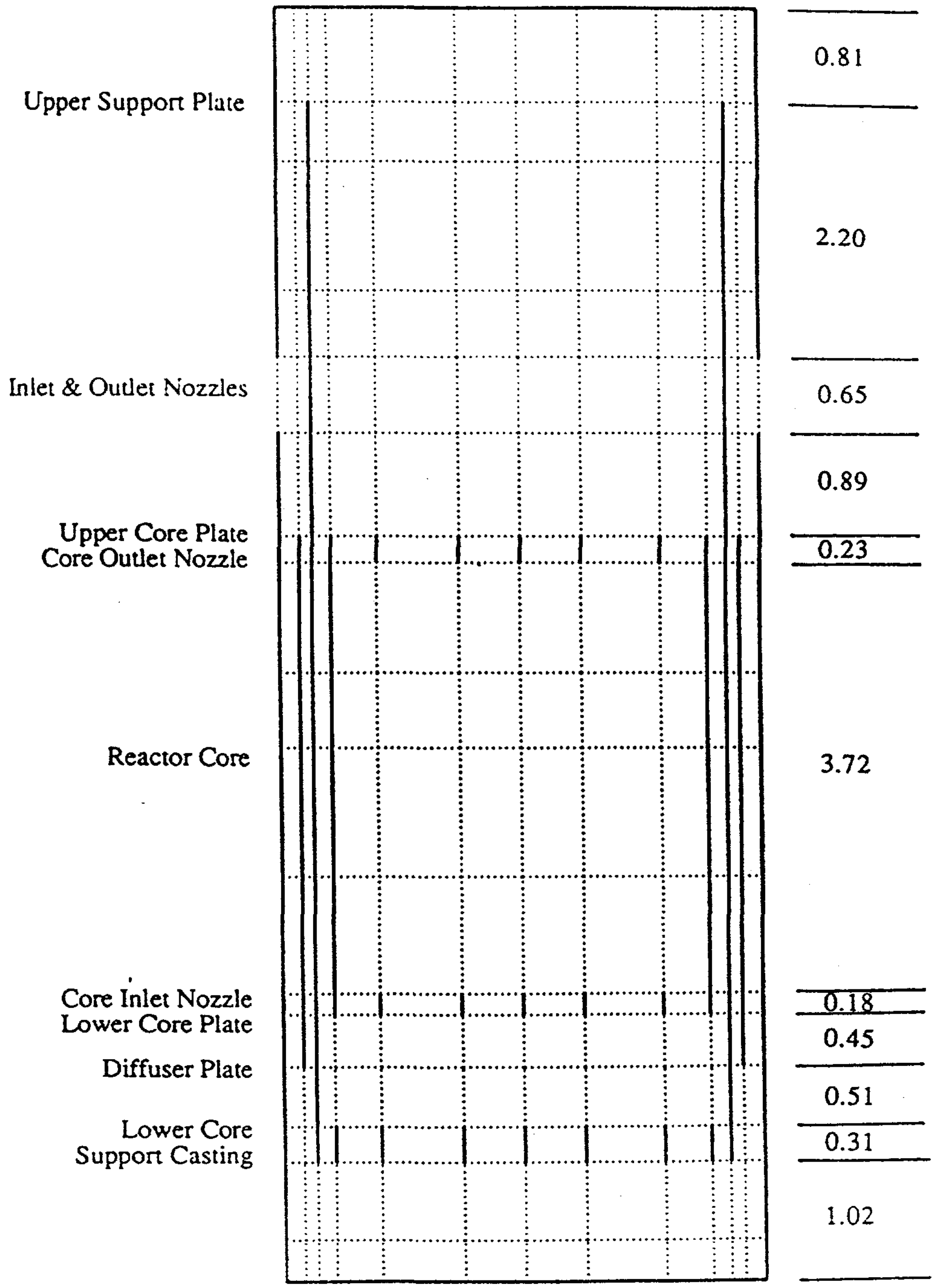

Fig. 6.. Vertical partitions of reactor vessel
(Dimensions in meters)

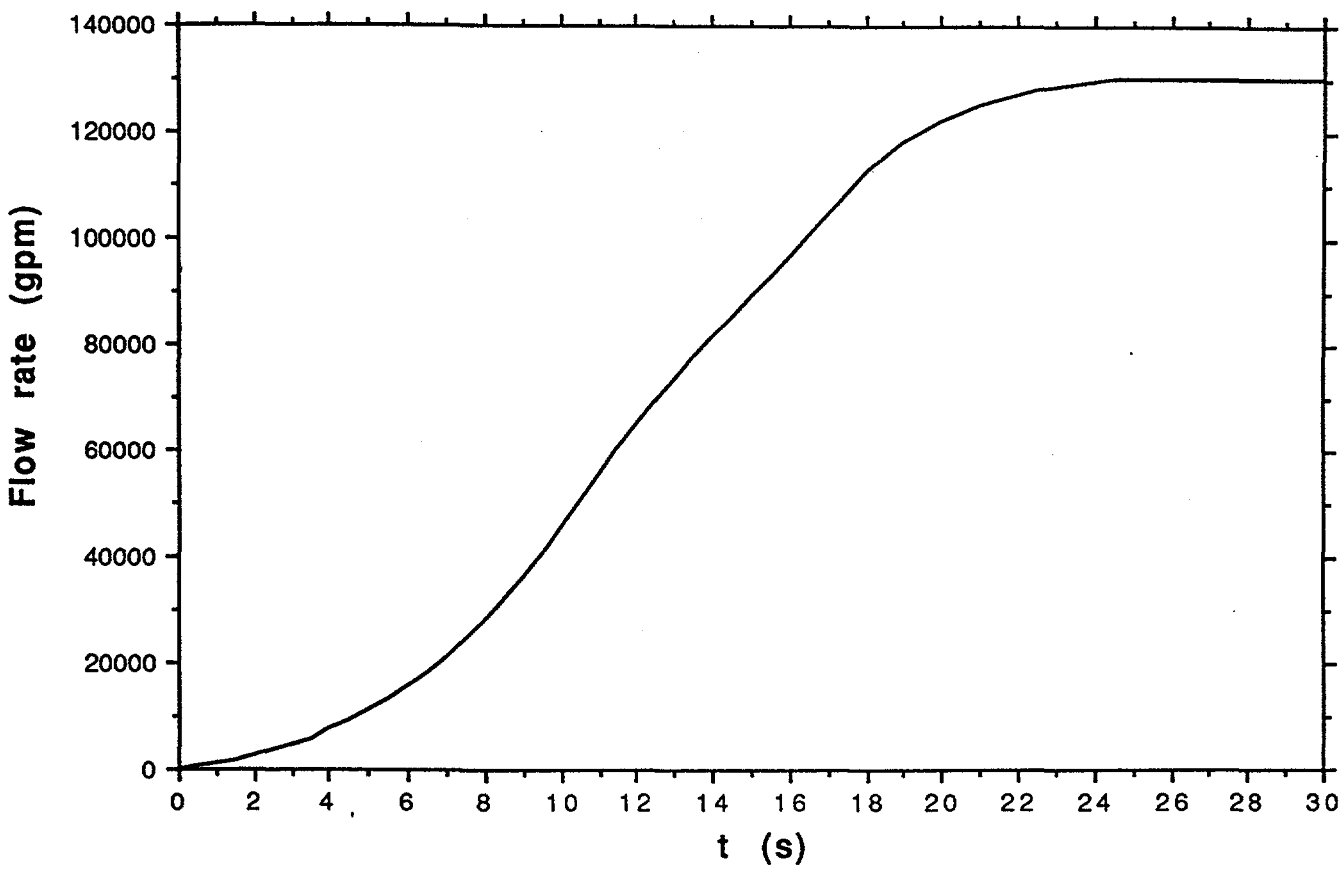

Fig. 7. Increase in flow rate with time at start of RCP

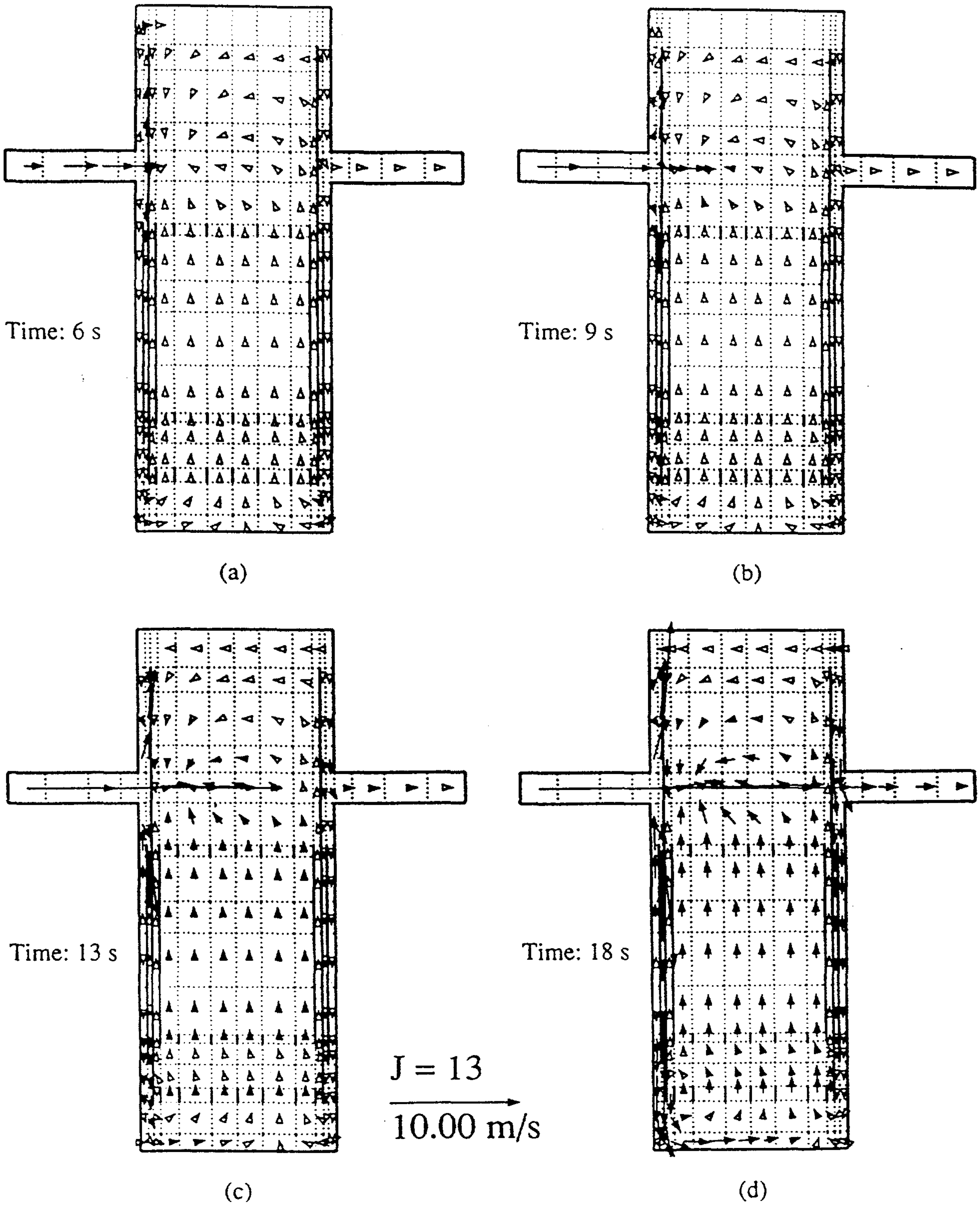

Fig. 8. Velocity distributions in cold legs and reactor vessel (vertical plane j=13) for isothermal-RCP-start calculation

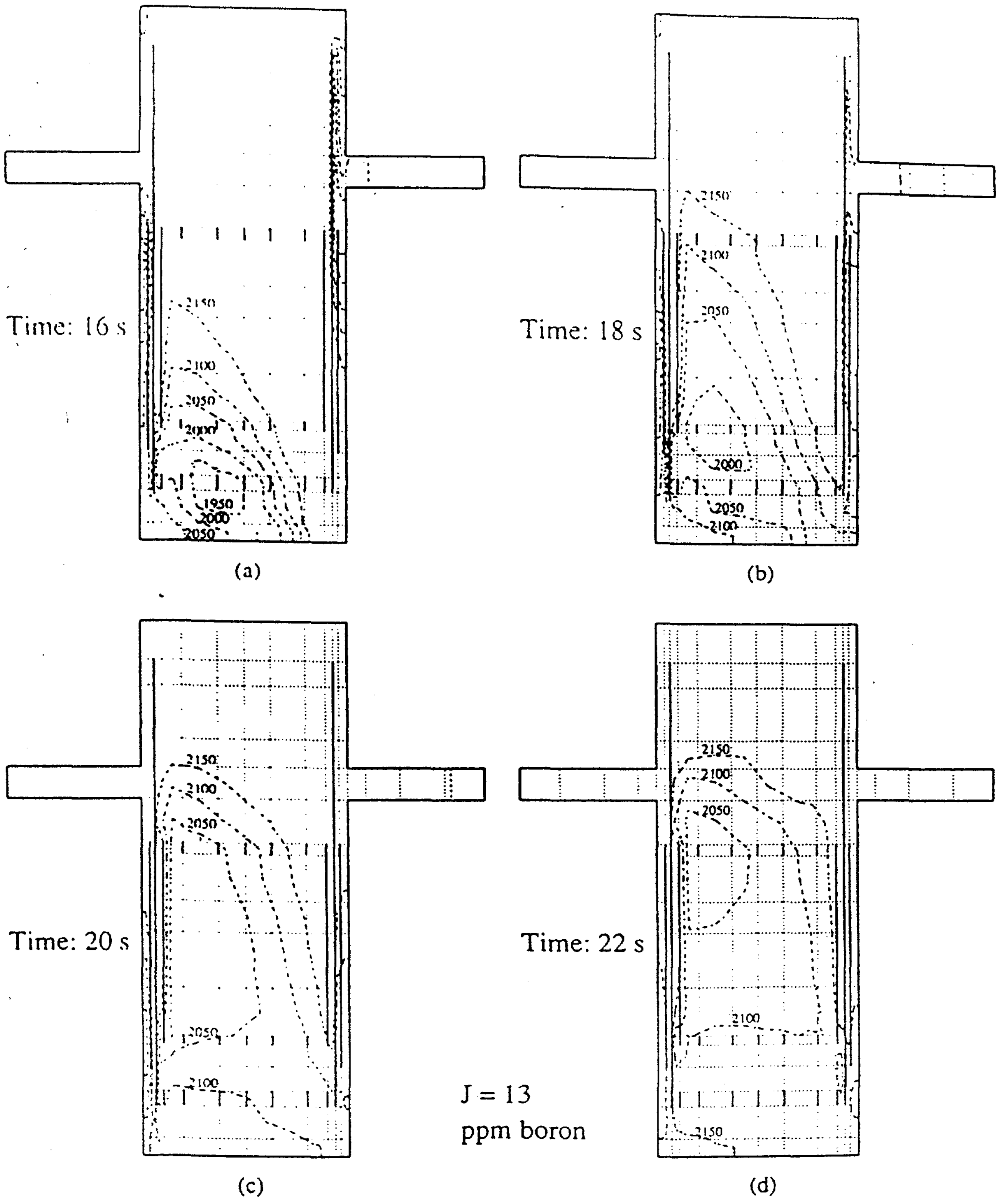

Fig. 9. Contours of boron concentration in reactor vessel (vertical plane j=13) for isothermal-RCP-start calculation

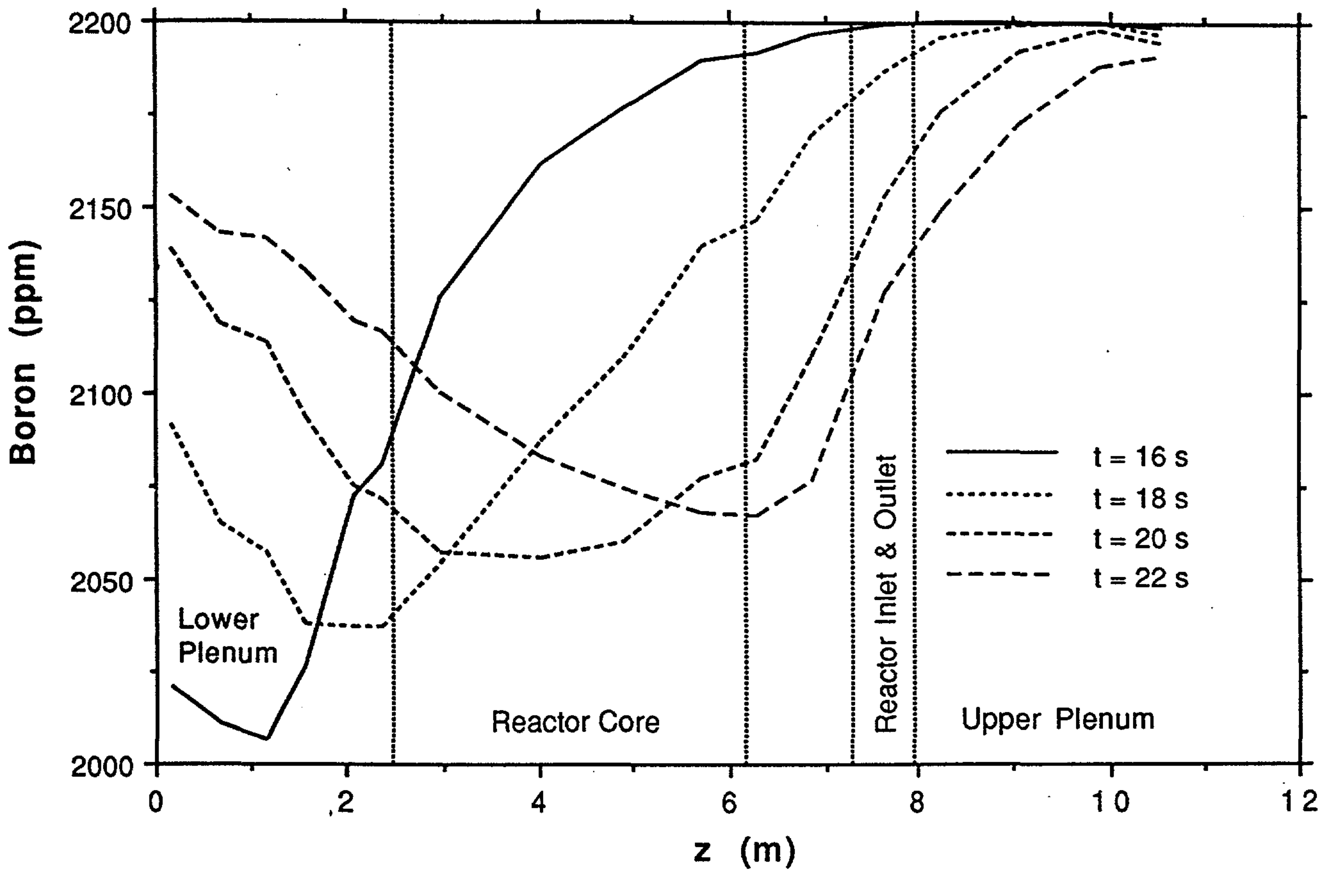

Fig. 10. Variation of boron concentration along axis of reactor vessel at 16, 18, 20, and 22 s into transient for isothermal-RCP-start calculation

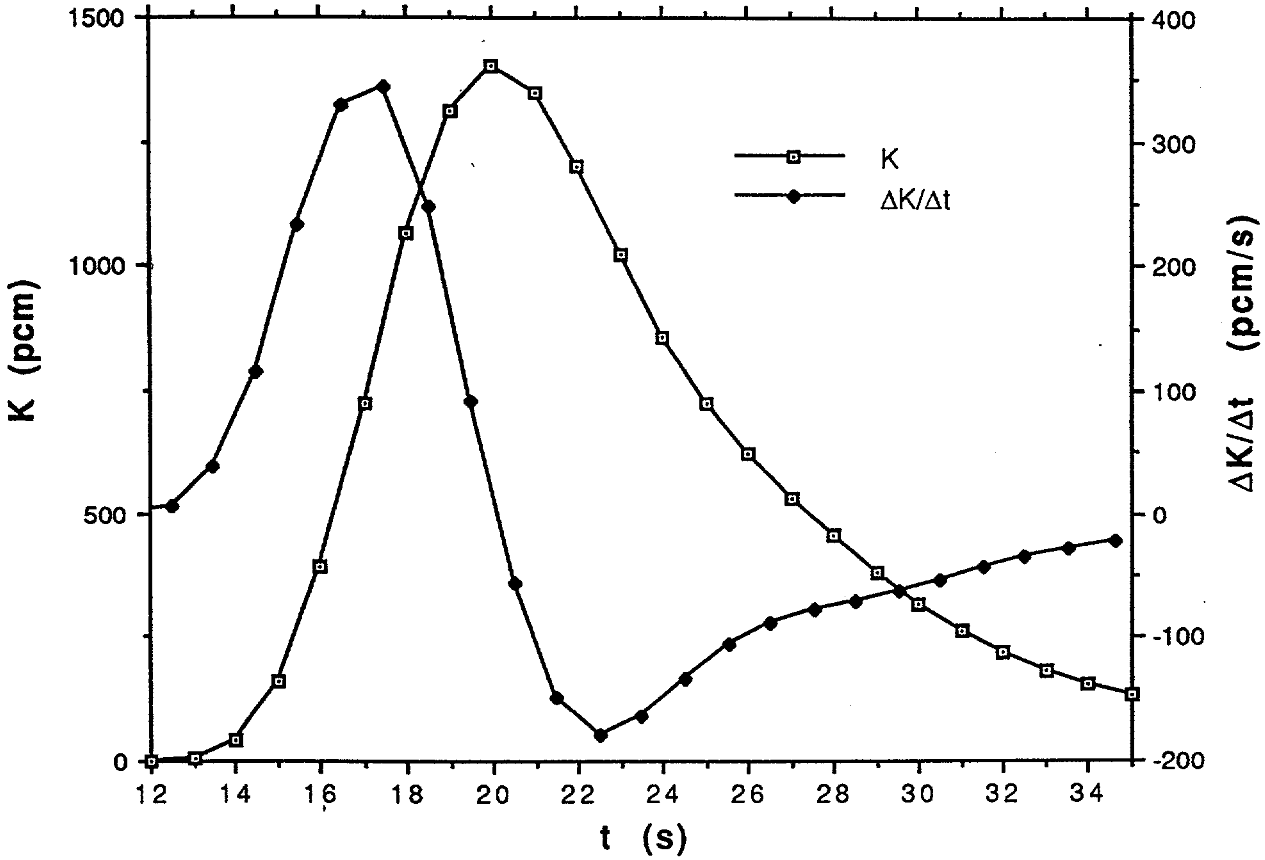

Fig. 11. Variation of mean reactivity and reactivity insertion rate with time in reactor core for isothermal-RCP-start calculation

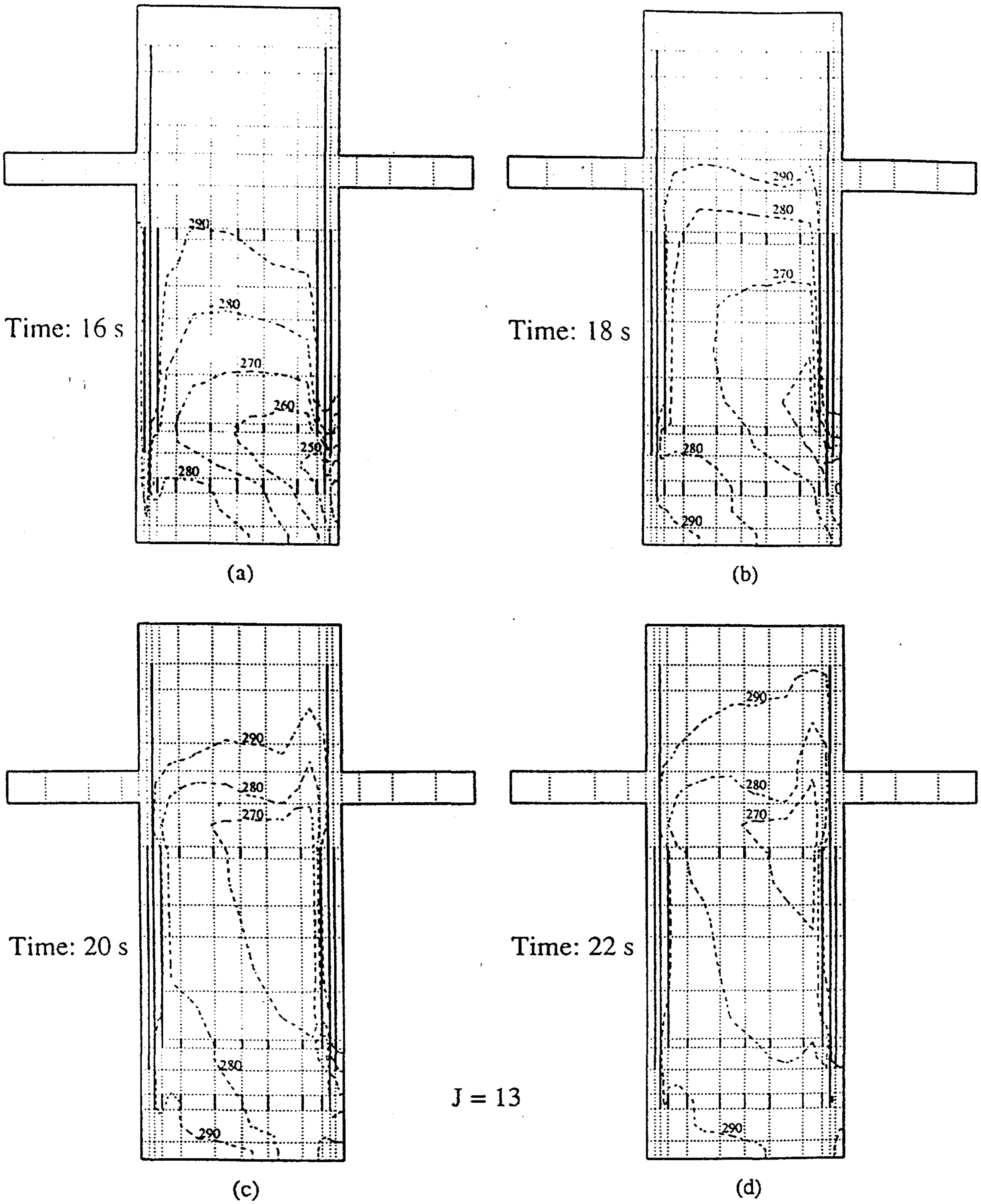

Fig. 12. Temperature (°C) contours in reactor vessel (vertical plane j=13) for hot-RCP-start calculation

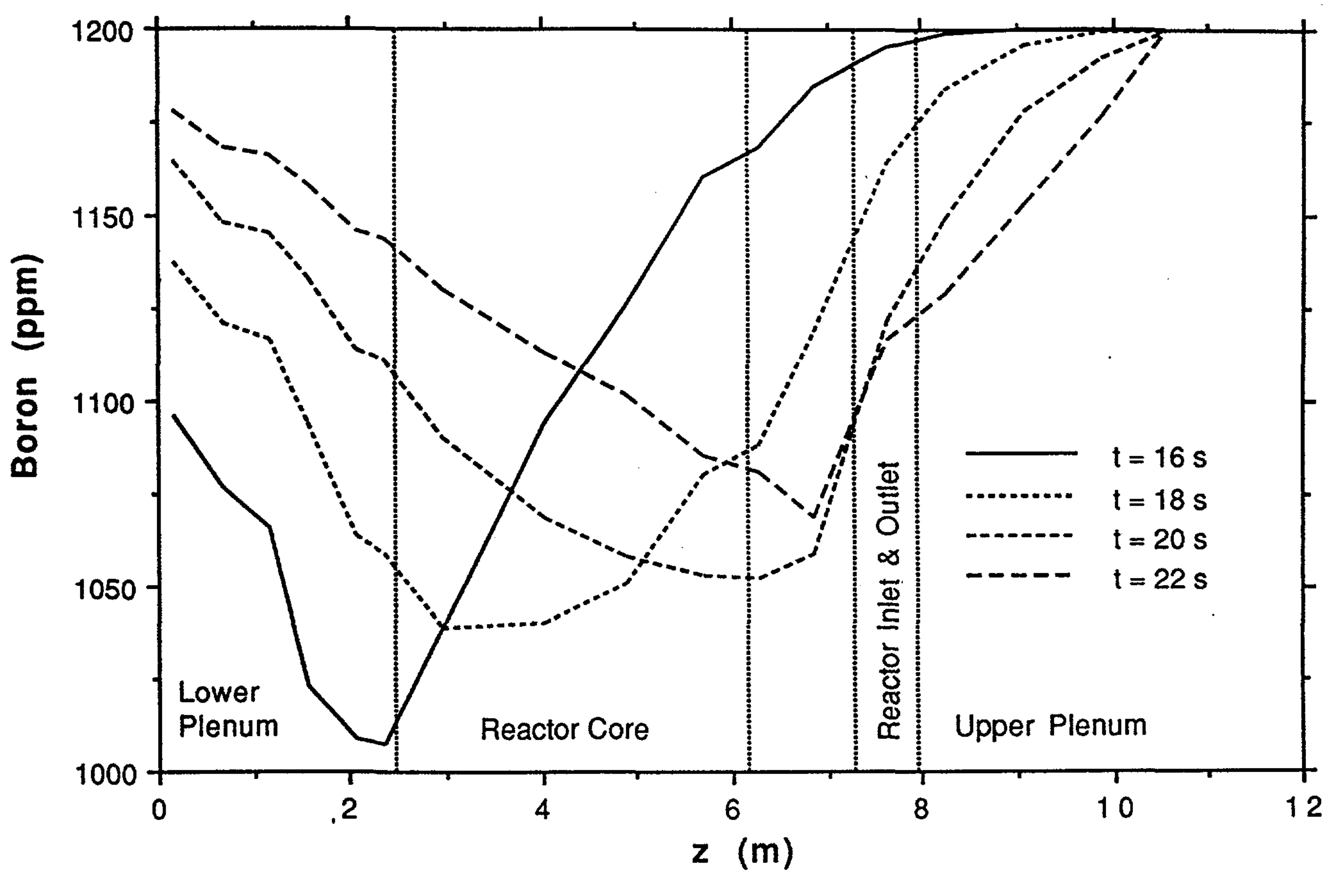

Fig. 13. Variation of mean boron concentration along axis of reactor vessel at 16, 18, 20, and 22 s into transient for hot-RCP-start calculation

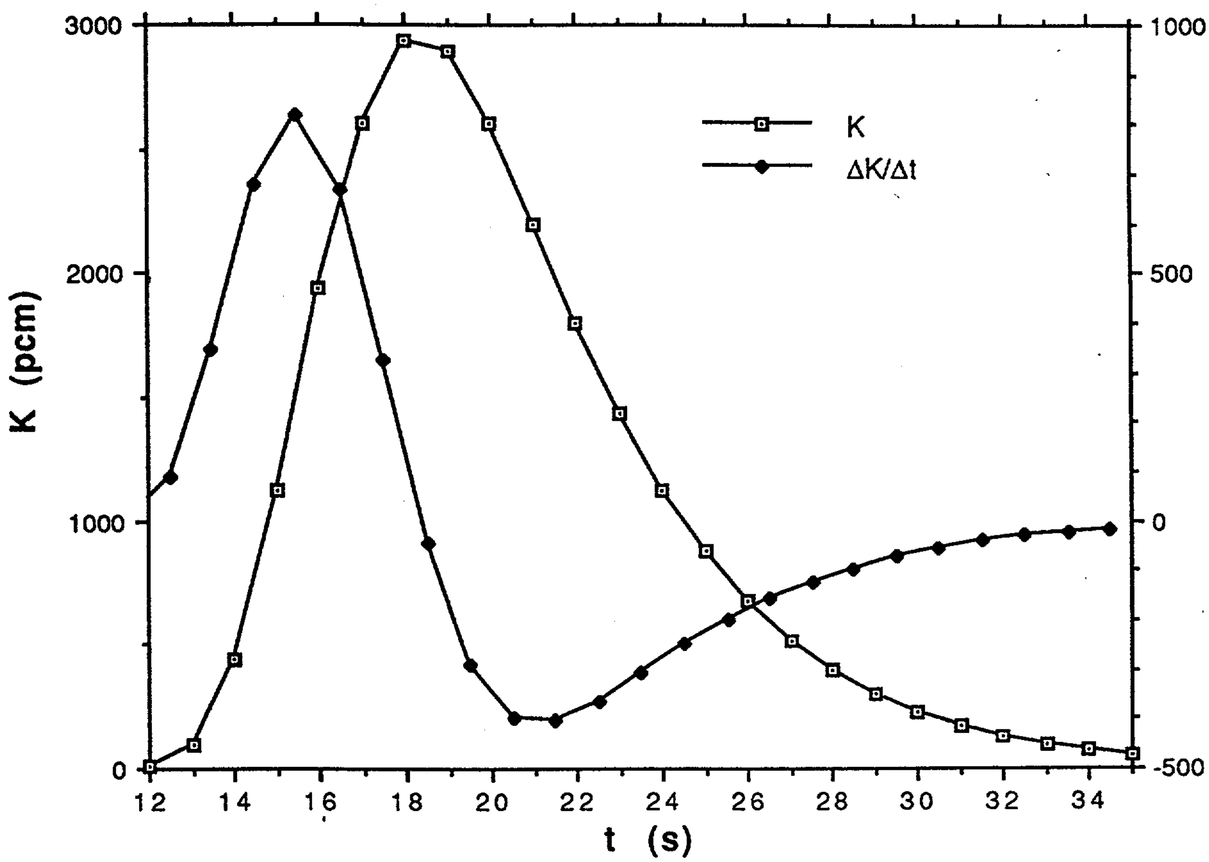

Fig. 14. Variation of mean reactivity and reactivity insertion rate with time in reactor core for hot-RCP-start calculation